Computers and Electronics in Agriculture 192 (2022) 106561

Contents lists available at ScienceDirect

Computers and Electronics in Agriculture

journal homepage: www.elsevier.com/locate/compag

Design of a variable-gain adjacent cross-coupled controller for coordinated motion of multiple permanent magnet linear synchronous motors

L. Li [a], Norbert Cheung [b], Guilin Yang [c], Chongchong Wang [c], P.F. Fu [b], G.C. Li [b], J.F. Pan [b,*]

[a] Heyuan Technology School, Heyuan 517000, China
[b] College of Mechatronics and Control Engineering, Shenzhen University, Shenzhen 518061, China
[c] Ningbo Institute of Materials Technology & Engineering, Ningbo 315201, China

ARTICLE INFO

Keywords:
Permanent magnet linear synchronous motor
Coordinated control strategy
Variable-gain adjacent cross-couple controller

ABSTRACT

Coordination position control of multi-motors systems is widely applied in agricultural and industrial fields that require high precision and synchronization among motors. Current adjacent cross-coupled control is unable to change the control gains as motor states are time-variant. The invariant gain compensation will inevitably weaken the coordinated control performance, especially in the presence of load disturbances. To solve this issue, this paper proposes a variable-gain adjacent cross-coupled controller. A sliding mode controller is adopted to cope with the disturbances and uncertainties for each single permanent magnet linear synchronous motor (PMLSM). The motor state of each PMLSM can be detected through system identification in real time. According to the motor states of the PMLSMs based on the system identification technique, a fuzzy position control algorithm is implemented for regulating the gain compensation. A consistent steady-state performance is subsequently maintained even with the existence of system uncertainties and load disturbances. It is proved from the experimental results that, compared with fixed-gain adjacent cross-coupled control scheme, the proposed controller has a better synchronization, a higher tracking accuracy and synergistic accuracy, under both no load and time-varying load conditions. For the variable-gain adjacent cross-coupled control, a position tracking error and a synergistic error within 7 μm and 8 μm can be achieved, respectively.

1. Introduction

As the fast demands increase for high-precision linear motion, the permanent magnet linear synchronous motor (PMLSM) can be found the applications in agricultural and industrial control fields. Apart from rotary-type motors with auxiliary mechanical devices like gears or ball screws, linear motors can drive the load directly without any extra transmissions (Zhang et al., 2019). Therefore, fast speed and high precision can be obtained. Nowadays, with the rapid growth of agriculture labor cost, autonomous agricultural machines are drawing more and more attention. Coordinated control based on multiple motors to achieve agricultural tasks has been applied (Zhang and Noguchi, 2017; Qiu et al., 2018; Kalmari et al., 2017). For example, in the multi-processing line in Fig. 1 (a), for a multiple linear-motors based planting processing line, there are three working procedures such as pesticide, water spraying, and chopping. Each task is required to be accomplished by the corresponding linear motor regarding the procedure and the linear motors are expected to work cooperatively instead of sequentially. It demands that the linear motors track the command position precisely and coordinate with each other to finish the entire work. Compared to the traditional sequenced working manner, the coordinated manner has the advantages of a faster operation time, higher efficiency, and the annihilation of accumulated errors, etc. (Rajamanickam et al., 2020).

To enhance the control capability of motion coordination, two main issues should be concerned. The first one is the tracking accuracy of the single PMLSM for a specified position. The traditional proportional integral differential (PID) controller is widely applied in the area of linear motor position tracking applications. The fixed gains from the PID controllers are not capable of a uniform performance in the presence of un-modeled uncertainties and load disturbances (Sharma and Palwalia, 2017). Fuzzy adaptive, fuzzy neural network and seeker optimization algorithm (SOA) combined with traditional PID are introduced to compensate the disadvantages from the PID control. In addition, different intelligent algorithms are adopted to achieve high-precision performance of the single PMLSM (Yong and Cong, 2019; Hu et al., 2019). Even though the above methods can realize high position

* Corresponding author.
E-mail address: pjf@szu.edu.cn (J.F. Pan).

https://doi.org/10.1016/j.compag.2021.106561
Received 25 December 2020; Received in revised form 11 October 2021; Accepted 7 November 2021
Available online 20 November 2021

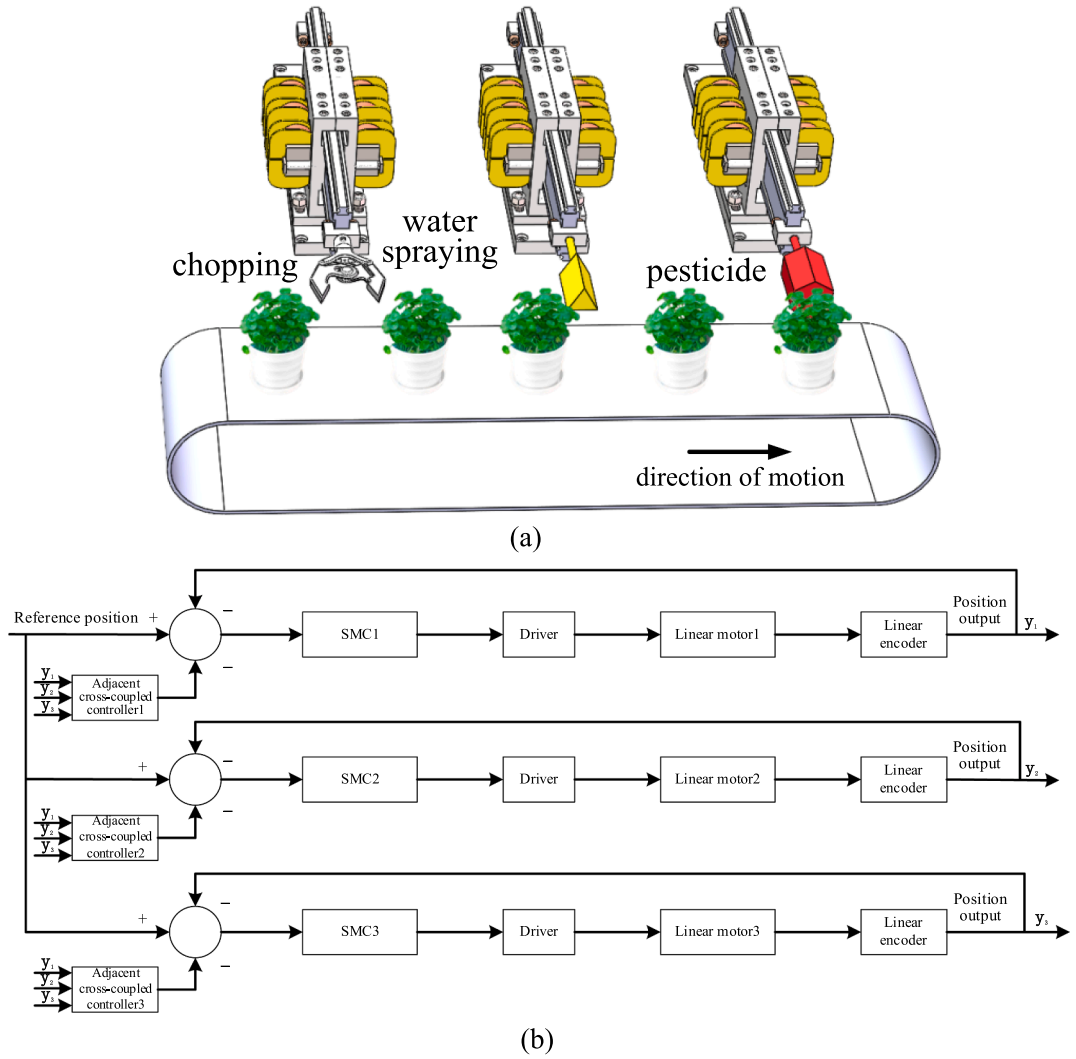

Fig. 1. Multi-motor coordinated control: illustration of multiple linear-motor based agriculture processing line (a) A multiple linear-motor based processing line (b) The structure of adjacent cross-coupled control.

tracking accuracy, these methods also lead to the problems of a complex arithmetic computation and the difficulty of real-time processing (Hu et al., 2019). Variable structure control can reduce the complexity of the controller and it has the characteristics of strong robustness and self-adjustment against un-modeled uncertainties and load disturbances (Li and Xie, 2010).

Another problem is the coordinated control precision of the multiple linear motors system. Current coordinated control can be divided into parallel control and master–slave control. In the parallel control structure, each motor follows the reference signal with no connection among motors. When any one motor malfunctions, the performance of the entire system will deteriorate. In the master–slave control structure, the master motor follows the reference signal, while the slave motors follow the master one, which will cause a large lagging among the slave motors. It is clear that both methods are not effective to solve the coordination task. Adjacent cross-coupled control which can achieve a better control performance has gradually replaced the former two coordinated methods, as shown in Fig. 1 (b). In the adjacent cross-coupled control structure, position errors from each motor and its two adjacent motors are subtracted mutually to form the synergistic errors, which are treated as the input of the coordinated controller. The coordinated controller is regulated by PID algorithm. The output of the coordinated controller is the gain compensation for each motor. The goal of the PID algorithm is to tune asymptotic convergence of the synergistic errors to zero through gain compensation scheme (Cao and Zhang, 2020; Huo and Poo, 2012). However, the gain compensation of the adjacent cross-coupled control cannot be changed based on the states of motor operation, which will inevitably weaken the coordinated control performance. To overcome the demerits from the fixed-gain adjacent cross-coupled control, a variable-gain adjacent cross-coupled control strategy is proposed in this paper. A fuzzy algorithm combined with system identification is introduced to the adjacent cross-coupled control strategy to correct fixed gain problems. The mover mass and viscous friction coefficient of each PMLSM which reflect the system variations can be detected by the system identification scheme. The reference position signal, the mover mass and viscous friction coefficient of each PMLSM are treated as the input of the fuzzy control algorithm (Kuang et al., 2019). Simultaneously, the output of the fuzzy control is the gain compensation, which can be regulated in real time accordingly. The variable gain has replaced the fixed gain from the PID algorithm of the adjacent cross-coupled control to compensate each motor adaptively.

Current research mainly focuses on the performance improvement for dual-PMLSM-based control applications. The research about three or above motors coordination motion control strategy is less involved. Article (El-Sousy, 2016) incorporates a mixed *H2 /H∞* controller, a self-organizing recurrent fuzzy-wavelet-neural-network controller (SORFWNNC) and a robust controller to achieve a high precision performance of a two-axis motion control system under uncertain plant

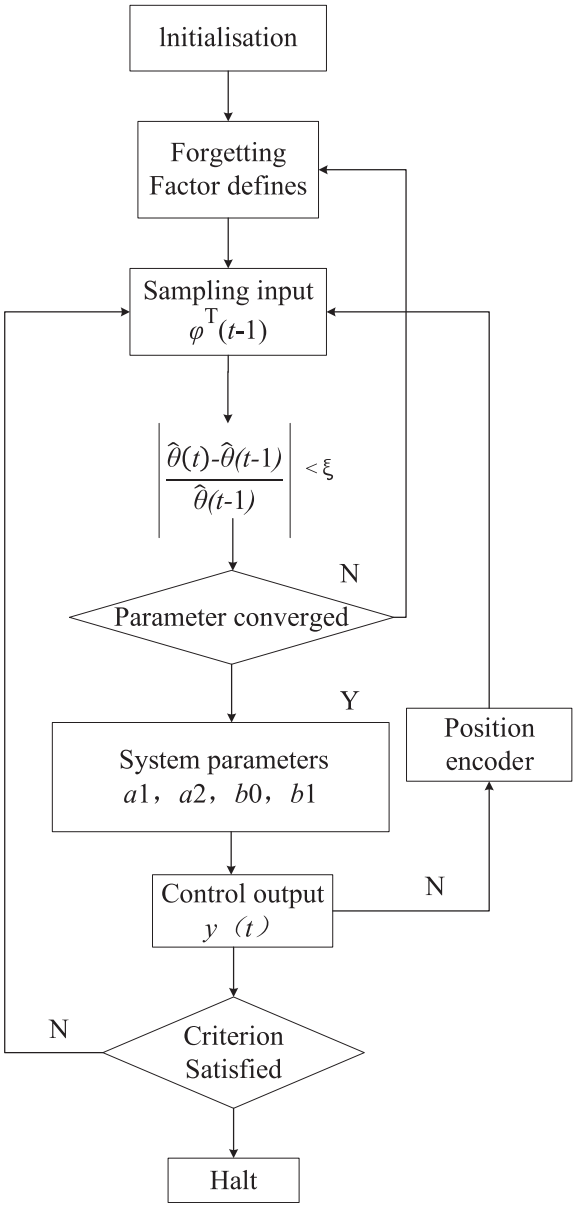

Fig. 2. The system identification flow chart.

Table 1
System identification results of three PMLSMs.

System identification	a_1	a_2	b_0	b_1
PMLSM1	−1.001	0.001312	0.0003293	3.280e-4
PMLSM2	−1.002	0.002891	0.0005730	5.738e-4
PMLSM3	−1.002	0.002853	0.0005702	5.711e-4

parameters and external disturbances. Article (Chou et al., 2012) proposes a complementary sliding mode control (CSMC) with Sugeno type fuzzy neural network (SFNN) compensator for the synchronous control of a dual linear motors servo system. Recently the consensus algorithm has been applied for second-order dynamics. The coordinated control based on the consensus algorithm has been proposed in the area of multiple flight vehicles for cooperative motion (Ren et al., 2016). Unfortunately, most of the research work is only focused on theoretical analysis and mathematical simulation, without considering the uncertain parameters and external disturbances. In addition, the coordinated motion control of multiple linear motors for cooperative agricultural applications can be rarely found in literature.

The contribution of this paper can be summarized as below. First, a variable structure control is implemented to reduce the complexity of the position controller for the single PMLSM and enhance the tracking accuracy with the characteristics of robustness and self-adjustment against un-modeled uncertainties and load disturbances. Second, the coordinated control strategy is introduced for the coordination motion position control system based on three PMLSMs in this paper. Third, the innovative variable-gain adjacent cross-coupled control strategy is implemented to obtain the run-time states of the motors by system identification and regulate gain compensation adaptively through fuzzy algorithm in real time. The variable gain derived from the proposed controller has replaced the fixed gain from the adjacent cross-coupled controller to compensate each motor adaptively. It can not only improve the synergistic accuracy, but also guarantee a high coordinated performance of the multiple linear motors coordination motion system, especially in the presence of un-modeled uncertainties and load disturbances. The effectiveness of the proposed controller is verified through theoretical simulation and times of experiments considering the uncertain parameters and external disturbances. The proposed controller is expected to be applied in the field of high-precision position coordination areas, especially in the cooperative agriculture applications, such as in trimming, sowing and watering, etc.

2. Mathematical model and controller design of the PMLSM

2.1. Mathematical model of the PMLSM

The system voltage balancing equation for each phase of the PMLSM can be described as

$$\begin{cases} u_d = R_s i_d + L_d \dfrac{di_d}{dt} - \dfrac{\pi}{p} v\varphi_q \\ u_q = R_s i_q + L_q \dfrac{di_q}{dt} + \dfrac{\pi}{p} v\varphi_d \end{cases} \tag{1}$$

where u_d, u_q, i_d, i_q, L_d, L_q, φ_d, and φ_q are d-q axis voltage, current, inductance and magnet flux linkage of the PMLSM, respectively. R_s is the phase winding resistance. p is the permanent magnet pole pitch. v is moving velocity of the mover.

The electromagnetic thrust equations can be described as

$$\begin{aligned} F_e &= \frac{3}{2}\frac{\pi}{p}\left[\varphi_f i_q + (L_d - L_q) i_d i_q\right] \\ &= \frac{3}{2}\frac{\pi}{p}\varphi_f i_q + \frac{3}{2}\frac{\pi}{p}(L_d - L_q) i_d i_q \end{aligned} \tag{2}$$

The control strategy of $i_d = 0$ is adopted for the current loop. Then Eq. (2) can be rewritten as

$$F_e = \frac{3}{2}\frac{\pi}{p}\varphi_f i_q = k_t i_q \tag{3}$$

where k_t is the electromagnetic force coefficient. Since k_t is a constant, it means that the electromagnetic thrust output is totally decided by i_q. We can realize direct control of the PMLSM through adjusting i_q.

The mechanical movement equation of the PMLSM is expressed as

$$M\frac{dv}{dt} = F_e - F_L - Bv \tag{4}$$

where M, F_L, B is mover mass, load disturbances and viscous friction coefficient, respectively (Xi et al., 2017).

2.2. Sliding mode controller of the PMLSM

Commonly, it is difficult for a traditional PID controller to achieve ideal control results when confronted to nonlinear control plant and

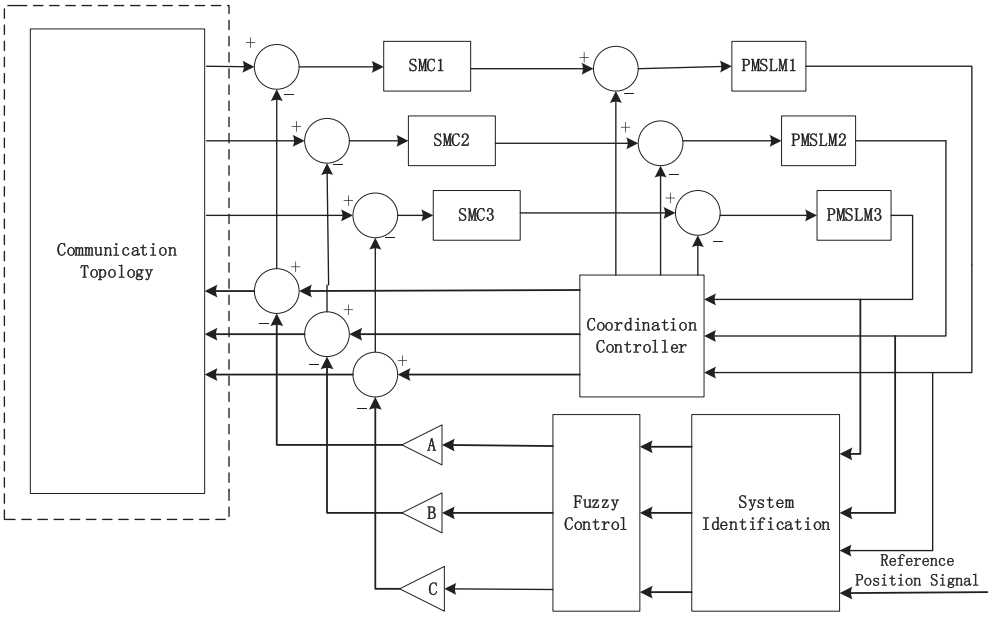

Fig. 3. The structure of the variable adjacent cross-coupled control.

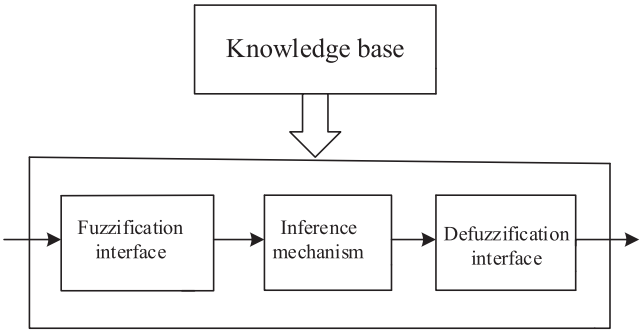

Fig. 4. The fuzzy logic algorithm block diagram.

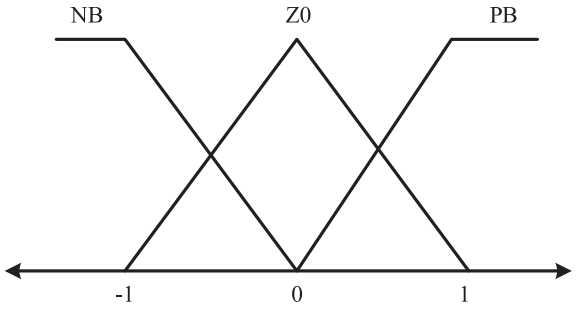

Fig. 5. The triangle membership function of input and output.

time-variant disturbances in a control system. As a type of variable structure control schemes, sliding mode control (SMC) is adopted in this paper to regulate the tracking response for each motor. SMC can cope with system parameter variations and external disturbances, which makes it suitable for the PMLSM motion system control. The mechanical movement equation of the PMLSM can be rewritten in the second-order form as

$$F_e = B\frac{dy}{dt} + M\frac{d^2y}{dt^2} + F_L \tag{5}$$

where y is displacement of the mover.

We choose $x=(x_1, x_2)^T$ as the state vector, where x_1 and x_2 represent the position and velocity of the PMLSM, respectively. i_q is adopted as the control input. The system can be described in the state-space equation form as

$$\begin{bmatrix} \dot{x}_1 \\ \dot{x}_2 \end{bmatrix} = \begin{bmatrix} 0 & 1 \\ 0 & -\frac{B}{M} \end{bmatrix} \begin{bmatrix} x_1 \\ x_2 \end{bmatrix} + \begin{bmatrix} 0 \\ \frac{K_t}{M} \end{bmatrix} i_q + \begin{bmatrix} 0 \\ -\frac{1}{M} \end{bmatrix} F_L \tag{6}$$

where F_L contains disturbances and un-modeled dynamics.

To design the sliding mode controller, a switching function is selected as

$$S(t) = C[x(t) - \int_0^t (A + BK)X(\tau)d\tau] = 0 \tag{7}$$

where C is a constant matrix and K is a gain matrix.

Considering the uncertainties in the PMLSM system, the proposed sliding mode controller based on the variable exponential approach law can be represented as

$$\begin{aligned} &\dot{S} = -\varepsilon|X|sgn(S) - \eta S \\ &\lim_{t\to\infty}|X| = 0, \eta > \varepsilon > 0 \end{aligned} \tag{8}$$

The symbol function often causes system chattering, and the switching surface surrounded by a boundary layer is introduced. The switching control vector u_s is thus defined as

$$u_s = ksat(\frac{s}{\sigma}) \tag{9}$$

where k is a constant. σ is thickness of the boundary layer. The saturation function $sat(\frac{s}{\sigma})$ has the following form as (Jiang et al., 2011)

$$sat(\frac{s}{\sigma}) = \begin{cases} \frac{s}{\sigma} & if \frac{s}{\sigma} \leqslant 1 \\ sgn(\frac{s}{\sigma}) & if \frac{s}{\sigma} > 1 \end{cases} \tag{10}$$

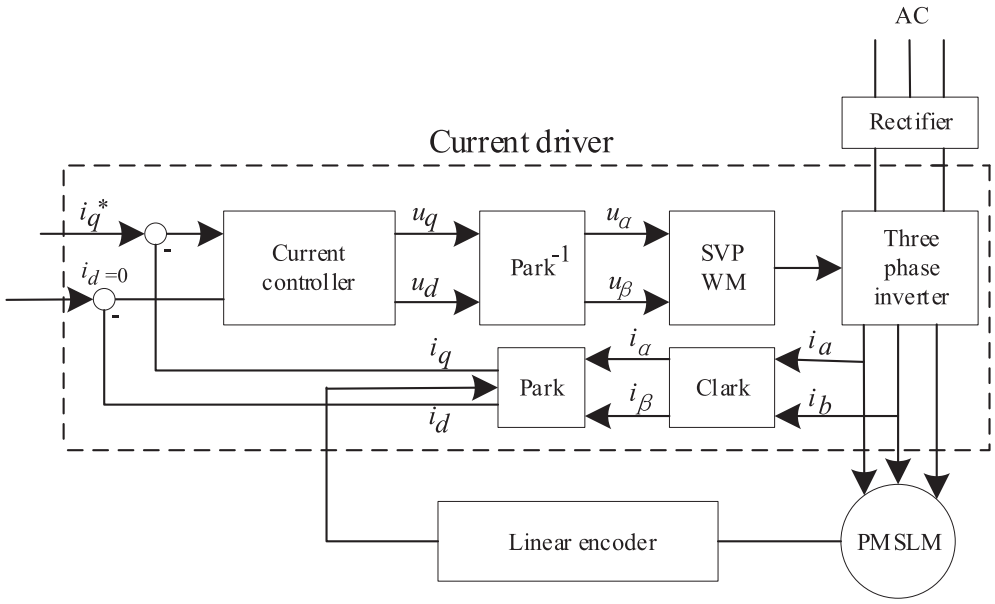

Fig. 6. The current and position loop control block diagram.

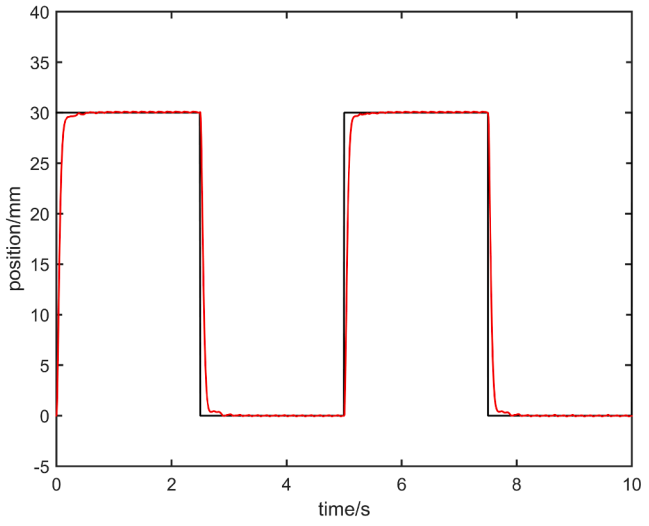

Fig. 7. Simulation results of the SMC for the PMLSM.

3. Coordinated control strategy of Multi-PMLSM

3.1. System identification base on recursive least square algorithm

Considering load disturbances $v(t)$, the PMLSM-based control system can be expressed with the motor required force $F(t)$ as the system input and the mover displacement $y(t)$ as the system output, respectively. The system output satisfies (11).

$$A(z^{-1})y(t) = B(z^{-1})F(t) + v(t) \tag{11}$$

where

$$\begin{cases} A(z^{-1}) = 1 + a_1 z^{-1} + a_2 z^{-2} \\ B(z^{-1}) = b_0 + b_1 z^{-1} \end{cases} \tag{12}$$

a_1, a_2, b_0, and b_1 are the system parameters to be identified. Eq. (11) can be denoted in a least square matrix form as

$$Y(t) = \varphi^T(t-1)\theta(t-1) + e(t) \tag{13}$$

where $\theta = [a_1, a_2, b_0, b_1]$, and $\varphi^T(t-1)$ stands for measurable values which consist of information of the force and displacement. $e(t)$ is white noise (Pan et al., 2013).

Let $\hat{\theta}(t)$ denotes the estimate of $\theta(t)$. The least square algorithm with the forgetting factor can be described as

$$\begin{pmatrix} \hat{\theta}(t) = \hat{\theta}(t-1) + K(t)[y(t) - \varphi^T(t)\hat{\theta}(t-1)] \\ K(t) = P(t-1)\varphi(t)[\varphi^T(t)P(t-1)\varphi(t) + \lambda]^{-1} \\ P(t) = \frac{1}{\lambda}[I - K(t)\varphi^T(t)]P(t-1) \\ 0 < \lambda \leqslant 1 \end{pmatrix} \tag{14}$$

where $P(t)$ is the covariance matrix. $K(t)$ is the adjusting gain. λ is referred as forgetting factor, which falls into the range of 0 to 1 and it reflects the convergence rate. The smaller λ is, the more quickly system parameters converge.

For the requirements of recursive calculation, the forgetting factor λ is set as 0.999, and the initial values are

$$\begin{cases} \hat{\theta}(0) = 0 \\ P(0) = I_{4\times4} \cdot r \end{cases} \tag{15}$$

If the relative error between the present and last step is less than ξ, which is a relatively small positive constant, the present estimated value can be regarded as correct. Then system identification can be terminated and the termination criterion is set as

$$\left| \frac{\hat{\theta}(t) - \hat{\theta}(t-1)}{\hat{\theta}(t-1)} \right| < \xi \tag{16}$$

The system identification flow chart is illustrated in Fig. 2.

System parameters a_1, a_2, b_0, and b_1 of three PMLSMs can be derived from online system identification as shown in Table 1.

We can also depict Eq. (5) with the mover mass M and viscous friction coefficient B as

$$G(z) = \frac{1}{B} \frac{(1 - e^{-\frac{B}{M}T_s})z}{z^2 - (1 + e^{-\frac{B}{M}T_s})z + e^{-\frac{B}{M}T_s}} \tag{17}$$

where T_s is the sampling time. By comparing Eq. (12) with Eq. (17), we can deduce M and B as

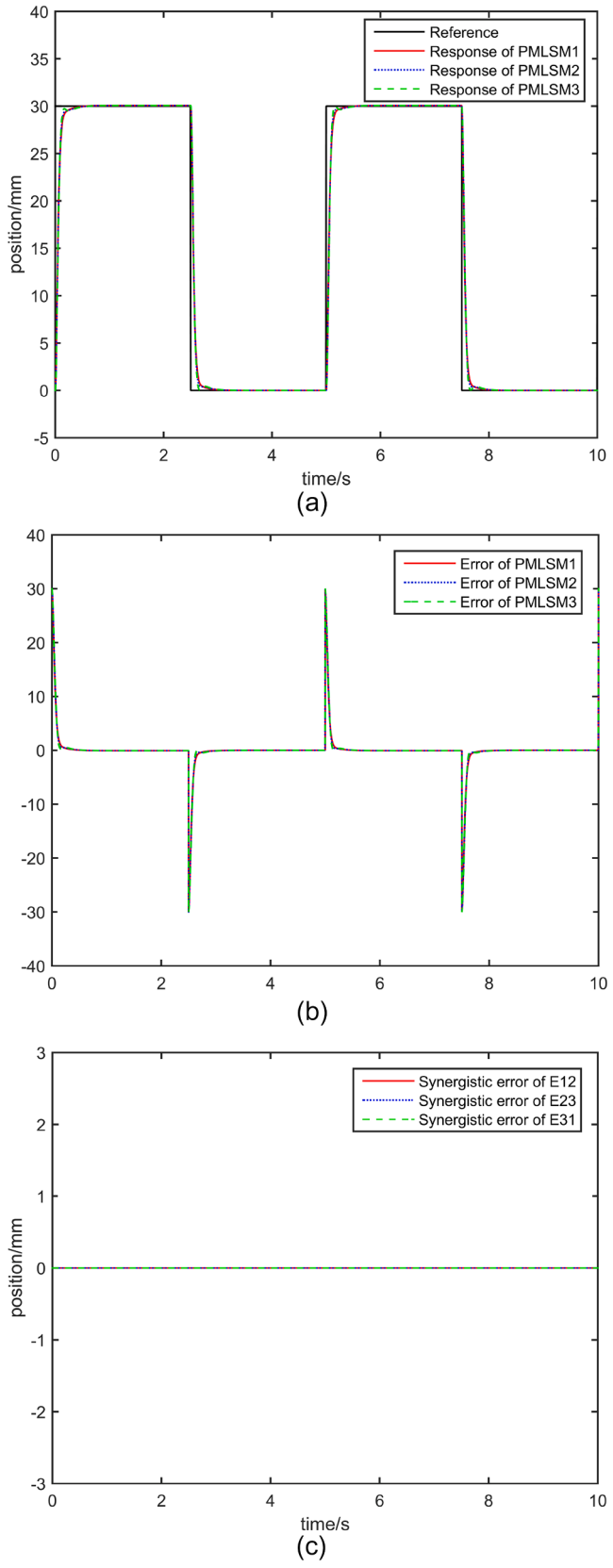

Fig. 8. Simulation results of the proposed variable-gain adjacent cross-coupled control strategy for the multi-PMLSM under no-load condition (a) Position tracking curves (b) Tracking error curves (c) Synergistic error curves.

$$\begin{cases} M = -\dfrac{b_1 T_s}{lna_1(2-a_2)} \\ B = \dfrac{b_1}{2-a_2} \end{cases} \tag{18}$$

3.2. Design of the variable-gain adjacent cross-coupled controller

In the adjacent cross-coupled control structure, the SMC is implemented to track the reference position signal for each PMLSM. Each motor follows the reference position command to produce the actual position response signal. The reference position subtracts the actual position to obtain the position tracking errors $e_1(t)$, $e_2(t)$, and $e_3(t)$ of three PMLSMs, which are treated as the input of the SMC. Position errors from each motor subtract the errors from its two adjacent motors to form the synergistic errors E_{12}, E_{23}, and E_{31}, which are defined as

$$\begin{cases} E_{12} = e_1(t) - e_2(t) \\ E_{23} = e_2(t) - e_3(t) \\ E_{31} = e_3(t) - e_1(t) \end{cases} \tag{19}$$

where $e_1(t)$, $e_2(t)$, and $e_3(t)$ are the position tracking errors of three PMLSMs, respectively.

The synergistic errors E_{12}, E_{23},and E_{31} are regarded as the input signals of the coordinated controller. The coordinated controller is regulated by PID algorithm. The output of the coordinated controller is the gain compensation for each motor. The goal of PID algorithm is to tune asymptotic convergence of synergistic errors to zero through gain compensation scheme. However, the gain compensation of the adjacent cross-coupled control cannot be changed based on the states of motor operation, which will inevitably weaken the coordinated control performance.

To overcome the disadvantage from the fixed-gain adjacent cross-coupled control, a variable-gain adjacent cross-coupled control strategy is proposed in this paper. Based on the adjacent cross-coupled control above, a fuzzy algorithm combined with system identification is introduced to correct the problems from the fixed gain control. The structure of the variable-gain adjacent cross-coupled controller is shown in Fig. 3. The mover mass M and viscous friction coefficient B of each PMLSM which reflect the system variations, can be detected by system identification. The mover mass M and viscous friction coefficient B of each PMLSM with the reference position signal are treated as the input of fuzzy control algorithm. Variables A, B, and C are changeable gain compensations, which are original from the output of fuzzy control and used to compensate the synergistic errors E_{12}, E_{23}, and E_{31}. In this way, the fixe-gain adjacent cross-coupled control has turned into the variable-gain adjacent cross-coupled control to compensate each motor in the presence of the system uncertainties and load disturbances (Yang et al., 2018).

The fuzzy logic algorithm block diagram can be found in Fig. 4, which has four principal modules. The knowledge base represents the knowledge in the form of a set of linguistic rules. The fuzzification interface manipulates the transformation of the inputs into fuzzy sets. The inference mechanism evaluates the relevant rules and proper inputs to the plant. The defuzzification interface transforms the fuzzy sets into corresponding outputs to the plant (Márquez-Vera et al., 2016).

The linguistic input variables are reference position U_0, mover mass M_1,M_2, M_3, and viscous friction coefficient B_1,B_2,B_3 of three PMLSMs. The linguistic output variables are gain compensation $output_1$,$output_2$, and $output_3$,which are able to change adaptively according to the motor running states.

The domain of input and output variables are {−1, 0, 1}, and the fuzzy subset is set as {NB, Z0, PB}. The input and output triangle membership functions are depicted in Fig. 5.

Next, we specify a set of linguistic rules which represent human's knowledge. Through times of data processing and multiple theoretical analysis, combined with users' experience, the relationships between

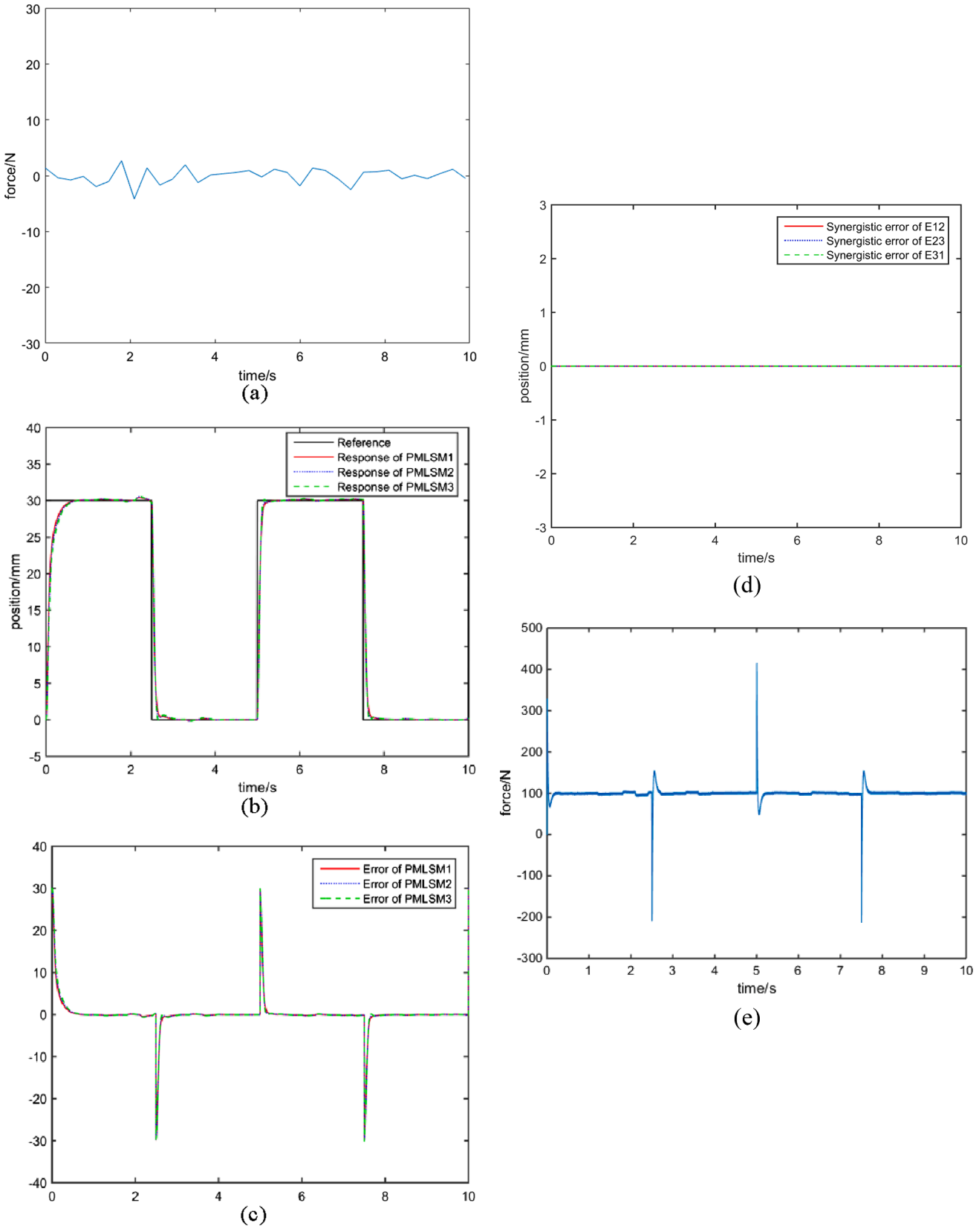

Fig. 9. Simulation results of the variable-gain adjacent cross-coupled control strategy for the multi-PMLSM under random load disturbance (a) Random load disturbance profile (b) Position tracking curves (c) Tracking error curves (d) Synergistic error curves(e) Force profile vs. time.

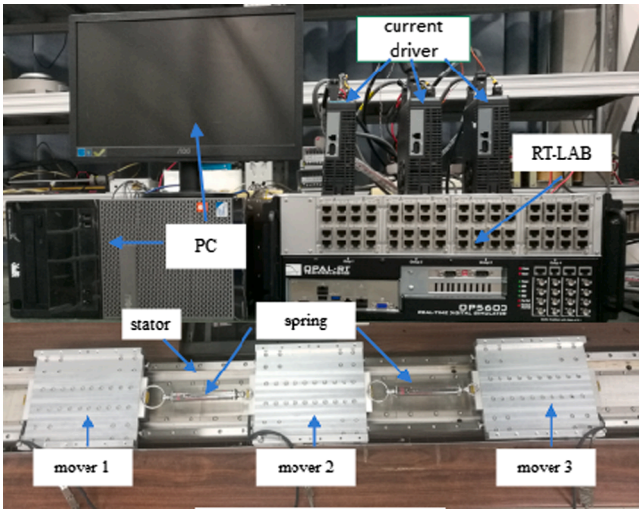

Fig. 10. Experimental setup.

input variables U_0,M_1,M_2,M_3,B_1,B_2,B_3 and output variables $output_1$, $output_2$, $output_3$ can be described as follows:

1) When the PMLSM is near to the reference position, in order not to deviate from the reference position, the gain compensation should be smaller.

2) When the mover mass of the PMLSM is smaller, to make the system have a good tracking capability, the gain compensation should be bigger.

3) When the PMLSM has a smaller viscous friction coefficient, to ensure a faster speed response, the gain compensation should be increased to an appropriate small value.

The Mamdani inference mechanism is introduced to deduce the linguistic rules. The final step is the defuzzification operation. Defuzzification is defined as the decoding of the fuzzy set information produced by inference mechanism into numeric fuzzy outputs. Here the center of gravity method is adopted to deal with the defuzzification. The center of gravity method is defined as

$$v_0 = \frac{\int_V v\mu_v(v)dv}{\int_V \mu_v(v)dv} \tag{20}$$

where $\int_V \mu_v(v)dv$ denotes the area under the membership function $\mu_v(v)$. v represents the center of the membership function. v_0 is referred as inference mechanism output.

3.3. The current and position loop control

The current and position double-loop control strategy is adopted. $i_d = 0$ is proposed to achieve the vector control for the current loop. It consists of the current controller based on proportion-integral (PI) algorithm, a space vector pulse width modulation (SVPWM), a power drive module, and a conversion module. The entire control block diagram is shown in Fig. 6. For the current loop, the core is vector control, which is treated as the inner loop. The actual position is obtained through linear encoder. The q-axis current i_q^* is given. By sampling the phase current of the PMLSM, the three phase current can be turned into i_q and i_d through CLARK and PARK transformation. The current command i_q^* minuses the actual current i_q and i_d minuses 0, which can produce voltage command u_q and u_d. After PARK reverse transformation, u_α and u_β are obtained. The SVPWM drives the three-phase inverter to realize the vector control of PMLSM (Pan et al., 2020). The position loop is treated as the outer loop. The deviation between reference position and the actual position of each motor is treated as input of the SMC. SMC is adopted to adjust the tracking error to improve the tracking accuracy of the PMLSM. The synergistic errors are introduced

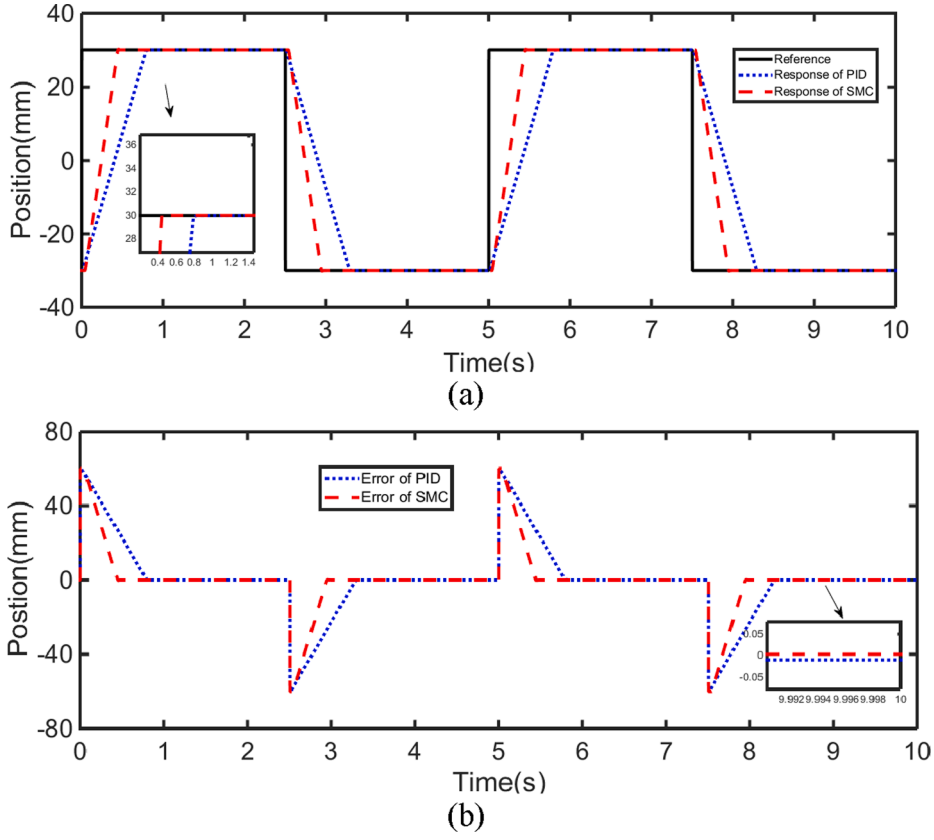

Fig. 11. Experimental results comparison between SMC and PID (a) Position tracking curves (b) Tracking error curves.

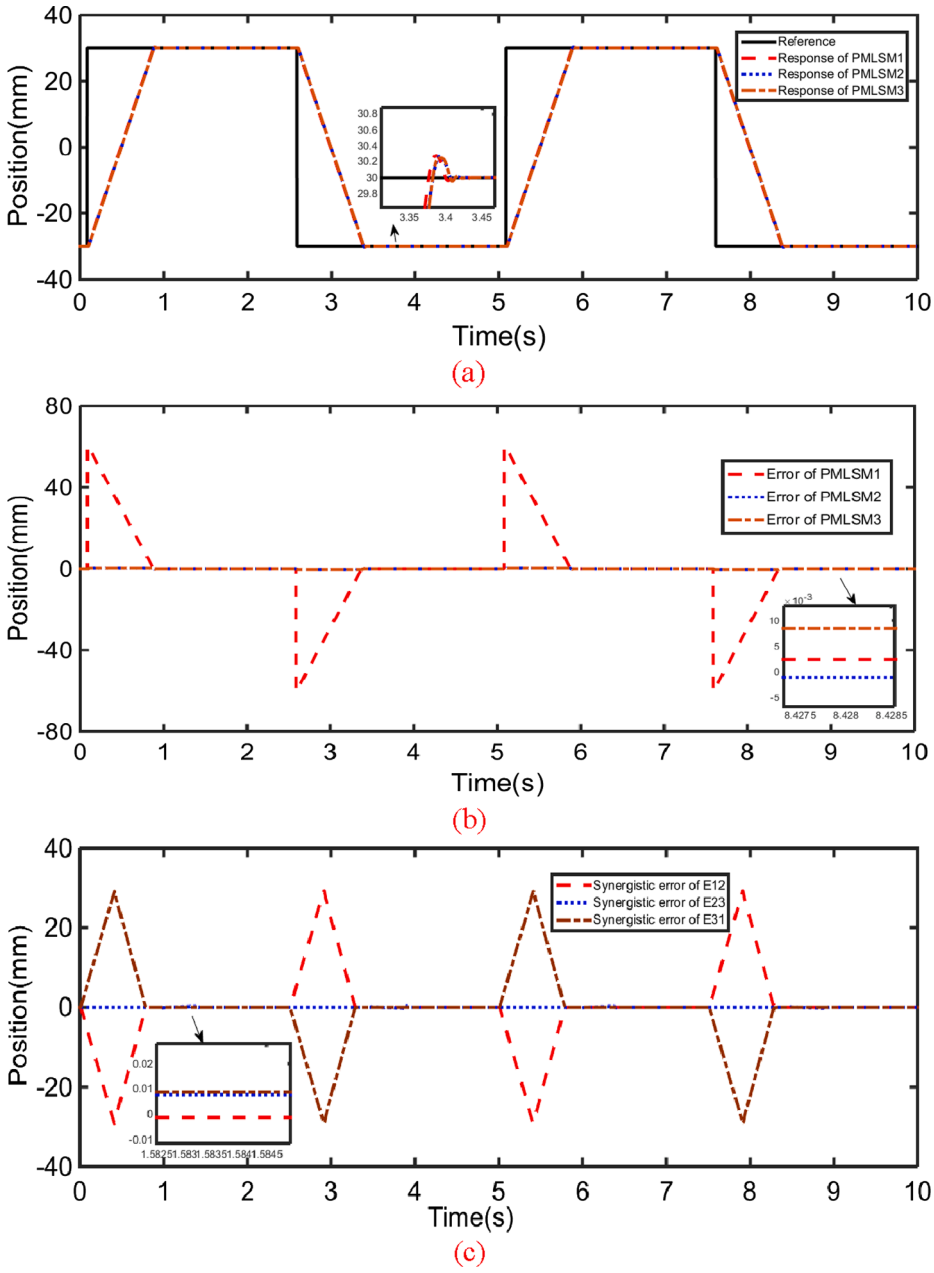

Fig. 12. Adjacent cross-coupled control strategy of multi-PMLSM under no-load condition (a) Position tracking curves (b) Tracking error curves (c) Synergistic error curves.

as the input signal of the coordinated controller to improve the synergistic accuracy.

4. Simulation and experimental results

4.1. Simulation results of the SMC for the PMLSM

In order to verify the effectiveness of the SMC proposed in this paper for the PMLSM, Matlab software is employed for the simulation analysis with the results shown in Fig. 7. It can be seen from Fig. 7 that the SMC exhibits a good position tracking performance, and the absolute steady-state position tracking error value is within 3 μm with no overshoot.

4.2. Simulation results of the variable-gain adjacent cross-coupled control strategy for multi-PMLSM

The simulation results of the proposed variable-gain adjacent cross-coupled control strategy for the multi-PMLSM can be found in Fig. 8. The simulation results demonstrate the performance of the proposed control strategy under no-load and random noise situations, respectively.

Under no-load condition, it can be concluded that three PMLSMs can track the reference position signal with a good synchronization behavior with a high response speed and no overshoot. Moreover, the absolute steady-state position tracking error values of three motors are the same and they are all controlled within 5 μm (Fig. 8 (b). The absolute steady-state synergistic error values of three motors are 0 μm (Fig. 8 (c)).

Fig. 9 demonstrates the dynamic response of the three PMLSMs under random load disturbance (Mean = 0, Variance = 2, Seed = 1), as shown in Fig. 9 (a). From Fig. 9 (b), though fluctuations occur from the

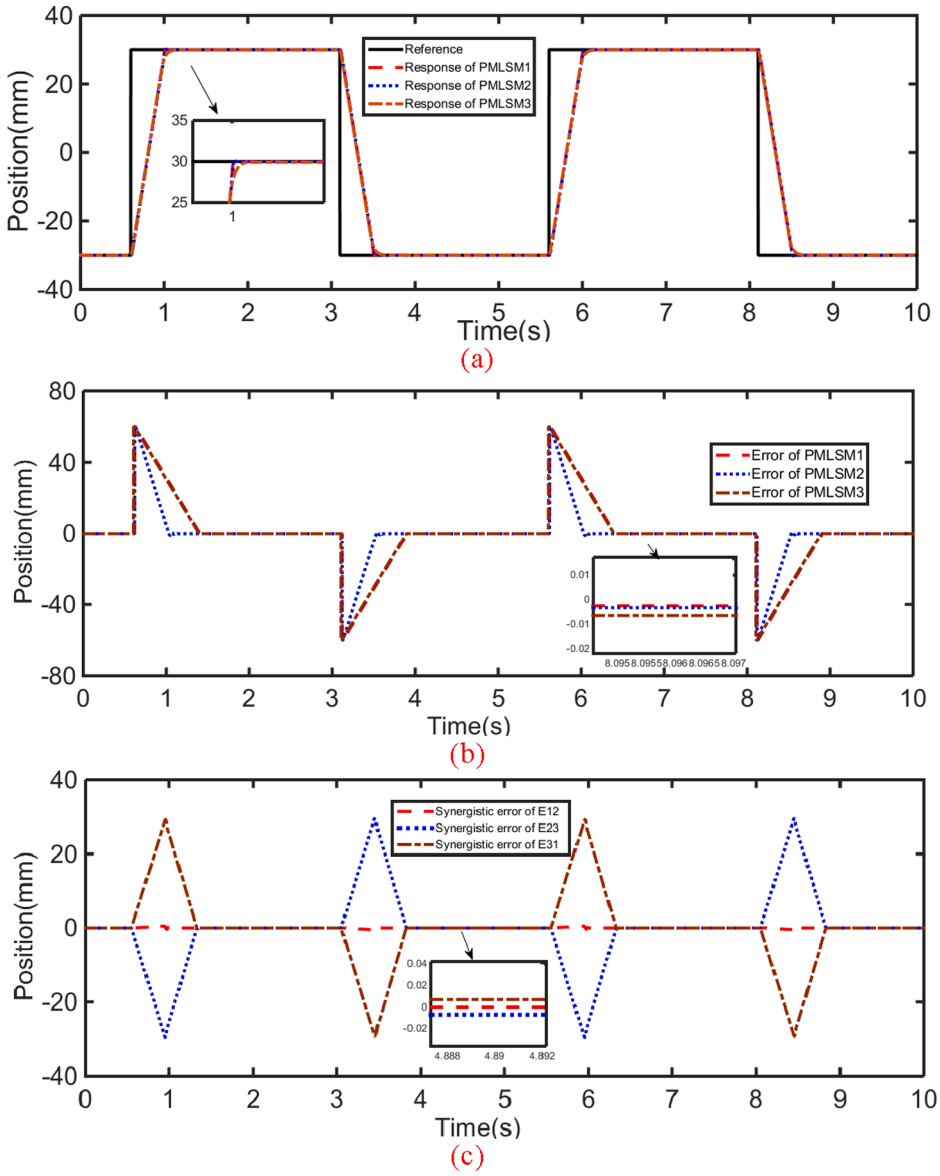

Fig. 13. Variable-gain adjacent cross-coupled control strategy of multi-PMLSM under no-load condition (a) Position tracking curves (b) Tracking error curves (c) Synergistic error curves.

Table 2
The performance comparison between two control strategies under no– load condition.

No-load condition	Adjacent cross-coupled control			Variable-gain adjacent cross-coupled control		
	M1	M2	M3	M1	M2	M3
tracking error	3 μm	4 μm	9 μm	2 μm	4 μm	6 μm
synergistic error	1 μm	8 μm	9 μm	<0.1 μm	7 μm	7 μm

dynamic response, the entire system is able to maintain a good synchronization performance with a high response speed. The absolute steady-state position tracking error values of three motors are the same within 7 μm, as shown in Fig. 9 (c). The absolute steady-state synergistic error values of three motors are 0 μm (Fig. 9 (d)). We can also find the results for the profiles of developed force vs. time from the motors in Fig. 9 (e).

4.3. Experiment setup

The experiment is conducted on the RT-LAB platform, which consists of upper machine (PC) and lower machine (RT-LAB OP5600). The control program is developed under the Matlab/Simulink environment which can be downloaded directly to the RT-LAB controller board.

The current and position double-loop control strategy is adopted to achieve the current and position control for the PMLSM. The inner current regulation can be performed by the commercial current driver, which is based on the PI algorithm with 20 kHz switching frequency and 1 kHz position loop sampling frequency (Pan et al., 2020). Three commercial current drivers are employed to output the required current for each motor. For the outer loop, three incremental linear encoders with a resolution of 1 μm are adopted to detect actual position signal of each PMLSM. Since the linear encoders are incremented ones, before motor operation, the zero point is set manually. A square wave signal with the frequency of 0.2 Hz and amplitude of 30 mm is set as the reference position signal. Fig. 10 shows the overall experimental setup.

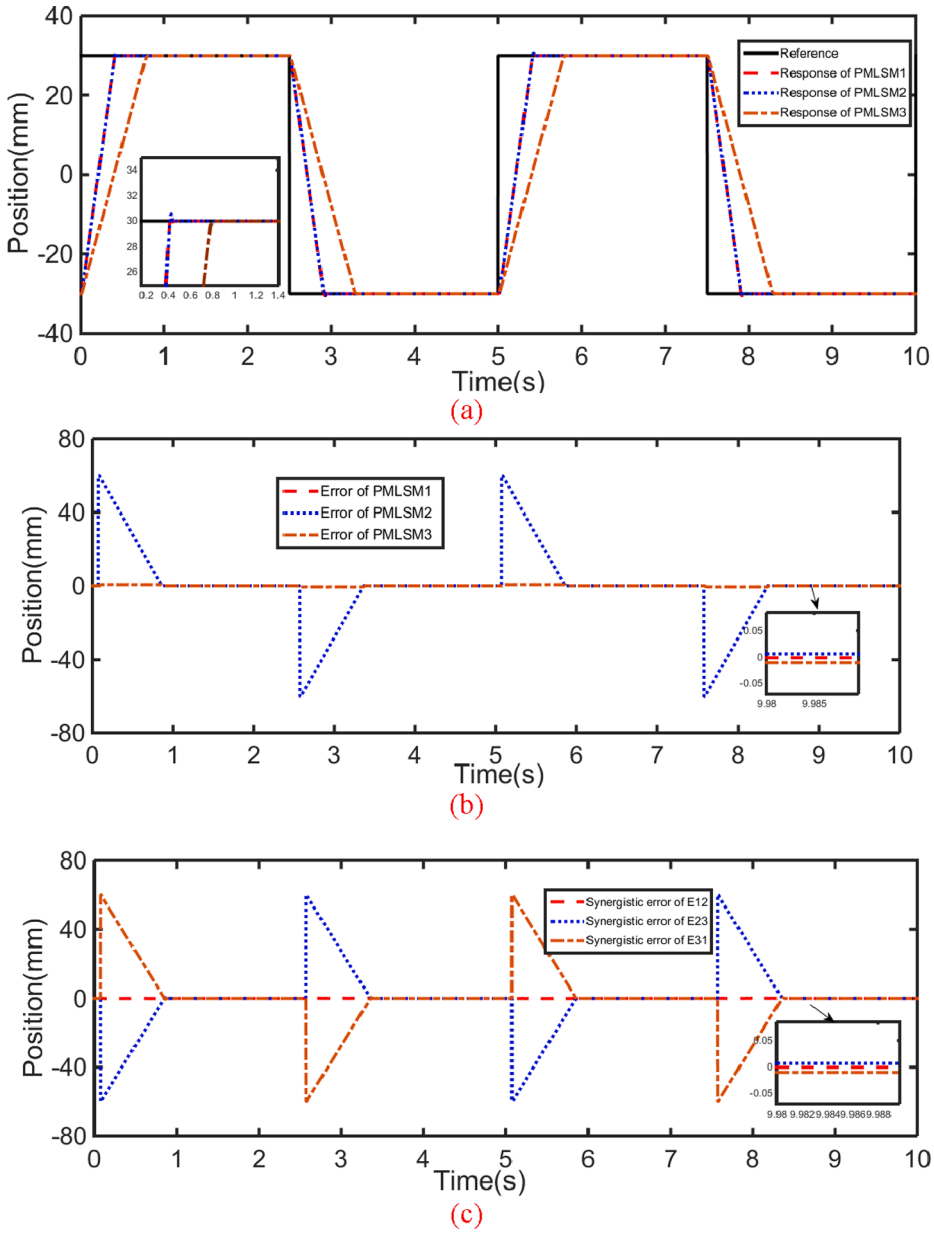

Fig. 14. Adjacent cross-coupled control strategy of multi-PMLSM under time-varying load condition (a) Position tracking curves (b) Tracking error curves (c) Synergistic error curves.

4.4. Experiment verification for the PMLSM

For the single PMLSM, to verify the superiority of the SMC over the traditional PID controller, the experiment of the single PMLSM system is carried out, and the experimental results are shown in Fig. 11.

Experimental results comparison between PID and SMC for position tracking response can be found in Fig. 11 (a). Although both controllers are capable of tracking the reference position signal, SMC exhibits a faster response speed and no overshoot. It can be seen from Fig. 11 (b) that an absolute steady-state position tracking accuracy of 3 μm can be achieved by the SMC while the accuracy from the PID controller is 6 μm. The experimental results are coincided with the simulation results. It is proved that SMC possesses a rapid response capability and a high tracking accuracy.

4.5. Experiment verification for multi-PMLSM

In the adjacent cross-coupled control structure, the SMC is implemented to enhance tracking accuracy of each motor. The coordinated controller which is regulated by PID algorithm outputs the fixed gain to compensate each motor. In the variable-gain adjacent cross-coupled control structure, based on the adjacent cross-coupled control above, a fuzzy algorithm combined with system identification is introduced to output variable gains to compensate each motor adaptively according to the motor running states. The experiment is implemented in the RT-LAB platform and the proposed control strategy is actuated at the interval of 1 ms. It can be guaranteed that the gain compensation scheme can be accomplished within 1 ms. Therefore, we can consider the control strategy is implemented to regulate gain compensation in real time.

For three PMLSMs, to verify the effectiveness of the variable-gain adjacent cross-coupled control strategy, the comparison experiment with the fixed-gain adjacent cross-coupled control strategy is carried out under no-load and time-varying load conditions, respectively.

CASE1: load is 0.

CASE2: load is a spring with the elastic coefficient of 10 N/mm.

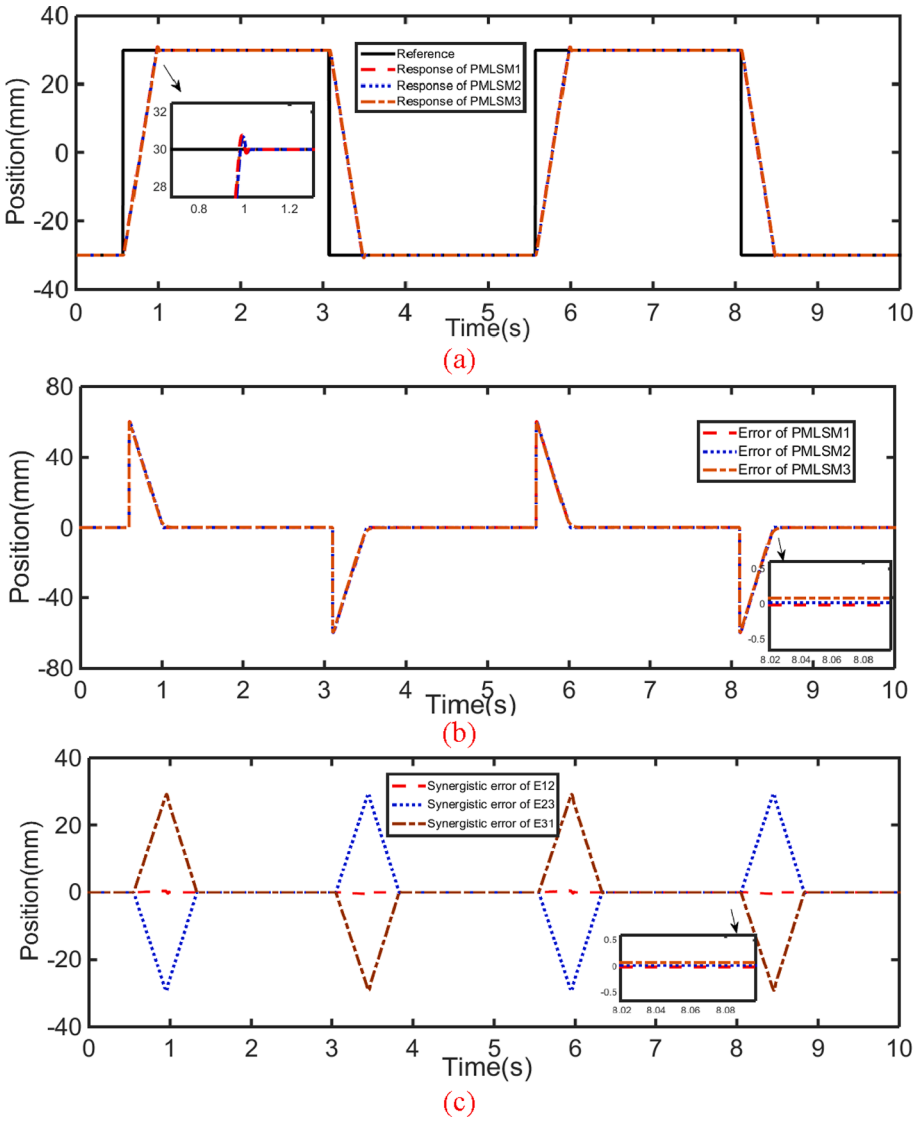

Fig. 15. Variable-gain adjacent cross-coupled control strategy of multi-PMLSM under time-varying load condition (a) Position tracking curves (b) Tracking error curves (c) Synergistic error curves.

Table 3
The performance comparison between two control strategies under time-varying load condition.

Time-varying load condition	Adjacent cross-coupled control			Variable-gain adjacent cross-coupled control		
	M1	M2	M3	M1	M2	M3
Tracking error	2 μm	7 μm	12 μm	4 μm	6 μm	7 μm
Synergistic error	8 μm	10 μm	18 μm	1 μm	7 μm	8 μm

For case 1, under no-load condition based on the adjacent cross-coupled control strategy, from Fig. 12 (a), we can see that three PMLSMs can track the position signal and have a good synchronization performance. It can be found from Fig. 12 (b) and (c) that the absolute steady-state position tracking error values of three motors are 3 μm, 4 μm, and 9 μm, respectively. The absolute steady-state synergistic error values of three motors are1μm, 8 μm, and 9 μm, respectively.

For case 1, under no-load condition based on the variable-gain adjacent cross-coupled control strategy, from Fig. 13 (a), we can see that three PMLSMs can track the reference position signal and have a better synchronization with no overshoot. We can also find from Fig. 13 (b) and (c) that based on the variable-gain adjacent cross-coupled control strategy, the absolute steady-state position tracking error values of each motor are 2 μm, 4 μm, and 6 μm, respectively. The absolute steady-state synergistic error values are less than 0.1 μm, 7 μm, and 7 μm, respectively. The response of three PMLSMs is consistent with the simulation results from Fig. 8 (a). The tracking and synergistic accuracy is a little lower than that from the simulation results, since the simulation is proposed in the idealized environment, neglecting electrical and mechanical imperfections from the machines and drives.

The performance comparison between two control strategies under no-load condition is shown in Table 2.

By comparing the above two control strategies under the no-load condition, it can be concluded that the variable-gain adjacent cross-coupled controller has a better synchronization performance with a higher response speed, no overshoot, and a better stability. Both the steady-state position tracking errors and the synergistic errors are smaller. The proposed control strategy can achieve a better steady-state position tracking accuracy and a higher synergistic accuracy than that from the fixed-gain adjacent cross-coupled controller.

For case 2, under time-varying load condition based on the adjacent cross-coupled control strategy, from Fig. 14 (a), we can see that PMLSM1 and PMLSM2 can track the reference position signal, but PMLSM3 has an

obvious out-of-step. PMLSM3 cannot track the reference position any more. It can be found from Fig. 14 (b) and (c) that the absolute steady-state position tracking error values of three motors are 2 μm, 7 μm, and 12 μm, respectively. The absolute steady-state synergistic error values of three motors are 8 μm, 10 μm, and 18 μm, respectively.

For case 2, under time-varying load condition based on the variable-gain adjacent cross-coupled control strategy, from Fig. 15 (a) we can see that three PMLSMs can track the reference position signal and keep a good better synchronization performance. We can also find from Fig. 15 (b) and (c) that based on the variable-gain adjacent cross-coupled control strategy, the absolute steady-state position tracking error values of each motor are 4 μm, 6 μm, and 7 μm, respectively. The absolute steady-state synergistic error values are 1 μm, 7 μm, and 8 μm, respectively. The experimental results coincide with the simulation results from Fig. 9 (a). Both the simulation and experiment results exhibit a faster response speed and a little overshoot. The tracking accuracy and synergistic accuracy is a little lower than that from the simulation.

The performance comparison between two control strategies under time-varying load condition is shown in Table 3.

By comparing the above two control strategies, we can deduce that the proposed variable-gain adjacent cross-coupled controller has a consistent good synchronization even under time-varying load condition, while the adjacent cross-coupled controller has an obvious out-of-step response and PMLSM3 cannot track the reference position anymore. Both the steady-state position tracking errors and the synergistic errors of the variable-gain adjacent cross-coupled control are within 8 μm, while the steady-state position tracking errors and the synergistic errors of the adjacent cross-coupled control are almost 20 μm. Compared with the results from the adjacent cross-coupled control, the proposed control algorithm not only can keep a consistent good synchronization, but also has a much higher steady-state tracking accuracy and synergistic accuracy while the adjacent cross-coupled control has malfunctioned under the time-varying load condition.

Under time-varying load condition, the adjacent cross-coupled controller is not capable of system change detection and gain compensation correction in real time and it leads to large disparity from the reference position. However, the proposed variable-gain adjacent cross-coupled controller is able to compensate external disturbances and dynamics with a uniform position tracking and coordination performance. The position tracking error and synergistic error values are within 7 μm and 8 μm, respectively. Experimental results prove that the proposed variable-gain adjacent cross-coupled controller has great superiority in the coordination motion control for multiple PMLSMs over the adjacent cross-coupled controller.

5. Conclusions

In this paper, a variable-gain adjacent cross-coupled controller for the multi-PMLSM system is proposed. The variations of motor uncertainties and external distances often result in a poor performance based on the fixed-gain adjacent cross-coupled control strategy. To maintain a good synchronization and ensure a consistent position tracking and coordination accuracy of the multi-PMLSM system, the variable-gain adjacent cross-coupled control strategy combines system identification with a fuzzy logic algorithm to detect system change and correct the gain compensation in real time. The effectiveness of the proposed controller under external load disturbances is verified by simulation and experimental results simultaneously. The proposed control strategy is expected to be applied in the field of high-precision position coordination areas, especially in the cooperative agriculture applications.

Declaration of Competing Interest

The authors declare that they have no known competing financial interests or personal relationships that could have appeared to influence the work reported in this paper.

Acknowledgment

This work was supported in part by the National Natural Science Foundation of China (U1913214) and in part by the International Collaborative Project of Shenzhen Government of China under GJHZ20200731095801004.

References

Cao, Y., Zhang, Z., 2020. Cross-Coupled Repetitive Control of a Compliant Nanomanipulator for Micro-Stereolithography. IEEE Access 8, 3891–3900.
Chou, Po-Huan, Chen, Chin-Sheng, Lin, Faa-Jeng, 2012. DSP-based synchronous control of dual linear motors via Sugeno type fuzzy neural network compensator. J. Franklin Inst. 349 (3), 792–812.
El-Sousy, Fayez F.M., 2016. El-Sousy, Intelligent mixed H2/H∞ adaptive tracking control system design using self-organizing recurrent fuzzy-wavelet-neural-network for uncertain two-axis motion control system. Appl. Soft Comput. 41, 22–50.
C. Hu, X. Sun, Z. Yang, G. Lei, Y. Guo and J. Zhu, A State Feedback Controller for PMSMs Based on Penalty Term Augmented Seeker Optimization Algorithm, 2019 22nd International Conference on Electrical Machines and Systems (ICEMS), 2019, pp. 1-4.
Huo, F., Poo, A.-N., 2012. Improving contouring accuracy by using generalized cross-coupled control. Int. J. Mach. Tools Manuf. 63, 49–57.
Jiang, J., Yingying, Y., 2011. Design of sliding mode controller for the position servo system Chinese Control and Decision Conference (CCDC). Mianyang 2011, 1016–1020.
Kalmari, J., Backman, J., Visala, A., 2017. Coordinated motion of a hydraulic forestry crane and a vehicle using nonlinear model predictive control. Comput. Electron. Agric. 133, 119–127.
Z. Kuang, X. Li, H. Wang, H. Gao and G. Sun. Precise Variable-Gain Cross-Coupling Contouring Control for Linear Motor Direct-Drive Table. 2019 American Control Conference (ACC). Philadelphia, PA, USA, 2019:5737-5742.
Li, F., Xie, H.-L., 2010. Sliding Mode Variable Structure Control for Visual Servoing System. Int. J. Autom. Comput. 7 (3), 317–323.
Márquez-Vera, Marco A., Ramos-Fernández, Julio C., Cerecero-Natale, Luis F., Lafont, Frédéric, Balmat, Jean-François, Esparza-Villanueva, Jorge I., 2016. Temperature control in a MISO greenhouse by inverting its fuzzy model. Comput. Electron. Agric. 124, 168–174.
Pan, J., Fu, P., Niu, S., Wang, C., Zhang, X., 2020. High-Precision Coordinated Position Control of Integrated Permanent Magnet Synchronous Linear Motor Stations. IEEE Access 8, 126253–126265.
Pan, J.F., Zou, Yu, Cao, Guangzhong, 2013. Adaptive controller for the double-sided linear switched reluctance motor based on the nonlinear inductance modelling. IET Electr. Power Appl. 7 (1), 1–15.
Qiu, Q., Fan, Z., Meng, Z., Zhang, Q., Cong, Y., Li, B., Wang, N., Zhao, C., 2018. Extended Ackerman Steering Principle for the coordinated movement control of a four wheel drive agricultural mobile robot. Comput. Electron. Agric. 152, 40–50.
Rajamanickam, A.K., Sanjay, M., Swetha, S., Ramprasath, R., 2020. Development of multipurpose agricultural machine. Mater. TodayProceedings. https://doi.org/10.1016/j.matpr.2020.11.094.
Ren, Chang-E, Chen, Long, Chen, C.L. Philip, Du, Tao, 2016. Tao Du, Quantized consensus control for second-order multi-agent systems with nonlinear dynamics, Neuro computing, Volume 175. Part A 175, 529–537.
Sharma, K., Palwalia, D.K., 2017. A modified PID control with adaptive fuzzy controller applied to DC motor. In: 2017 International Conference on Information, Communication, Instrumentation and Control (ICICIC), pp. 1–6.
Xi, Jingsi, Dong, Zeguang, Liu, Pinkuan, Ding, Han, 2017. Modeling and identification of iron-less PMLSM end effects for reducing ultra-low-velocity fluctuations of ultra-precision air bearing linear motion stage. Precis. Eng. 49, 92–103.
Yang, R., Wang, M., Li, L., Zhang, C., Jiang, J., 2018. Robust Predictive Current Control With Variable-Gain Adaptive Disturbance Observer for PMLSM. IEEE Access 6, 13158–13169.
S. Yang and C. Gong, Application of Fuzzy Neural Network PID Algorithm in Oil Pump Control, 2019 International Conference on Computer Network, Electronic and Automation (ICCNEA), 2019, pp. 415-420.
Zhang, W., Nan, N., Yang, Y., Zhong, W., Chen, YangQuan, 2019. Force ripple compensation in a PMLSM position servo system using periodic adaptive learning control. ISA Trans. 95, 266–277.
Zhang, C., Noguchi, N., 2017. Development of a multi-robot tractor system for agriculture field work, Computers and Electronics in Agriculture, Volume 142. Part A 142, 79–90.